Solid-State and Solution Structural Studies of 4-{[*C*(*E*)]-1*H*-Azol-1-ylimino)methyl}pyridin-3-ols

by **Dionisia Sanz***[a]), **Almudena Perona**[a]), **Rosa M. Claramunt**[a]), **Elena Pinilla***[b]), **M. Rosario Torres**[b]), and **José Elguero**[c])

[a]) Departamento de Química Orgánica y Bio-Orgánica, Facultad de Ciencias, UNED, Senda del Rey 9, ES-28040 Madrid (fax: +34 913988372; e-mail: dsanz@ccia.uned.es)

[b]) Departamento de Química Inorgánica, Laboratorio de Difracción de Rayos X, Facultad de Ciencias Químicas, Universidad Complutense, ES-28040 Madrid (e-mail: epinilla@quim.ucm.es)

[c]) Instituto de Química Médica (CSIC), Centro de Química Orgánica 'Manuel Lora Tamayo', Juan de la Cierva 3, ES-28006 Madrid

The new *N*-salicylideneheteroarenamines **1**–**4** were prepared by reacting the biologically relevant 3-hydroxy-4-pyridinecarboxaldehyde (**5**) with 1*H*-imidazol-1-amine (**6**), 1*H*-pyrazol-1-amine (**7**), 1*H*-1,2,4-triazol-1-amine (**8**), and 1*H*-1,3,4-triazol-1-amine (**9**). Solution ^{1}H-, ^{13}C-, and ^{15}N-NMR were used to establish that the hydroxyimino form **A** is the predominant tautomer. A combination of ^{13}C- and ^{15}N-CPMAS-NMR with X-ray crystallographic studies confirms that the same form is present in the solid state. The stabilities and H-bond geometries of the different forms, tautomers and rotamers, are discussed by using B3LYP/6-31G** calculations.

1. Introduction. – *N*-Salycilidenearenamines (salicylidene = (2-hydroxyphenyl)-methylene) show hydroxyimino **A**/oxoenamino **B** tautomerism, due to a proton-transfer process both in solution and in the solid state (*Scheme 1*) [1][2].

Scheme 1

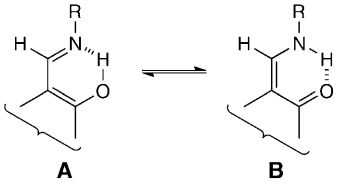

It has been established that in aromatic *Schiff* bases of *o*-hydroxybenzaldehydes, the equilibrium, normally favoring **A**, is shifted toward tautomer **B** when increasing the polarity of the solvent or the electron-withdrawing ability of the substituent R [1]. However, the N–H form **B** is rarely found [2][3].

Recently, we have been involved in the study of aromatic *Schiff* bases derived from 3-hydroxypyridine-4-carboxaldehyde (**5**) in an attempt to model the H-bonded structure of the cofactor pyridoxal-5′-phosphate (= 3-hydroxy-2-methyl-5-[(phosphonooxy)methyl]pyridine-4-carboxaldehyde) intervening in various enzymatic transformations of amino acids [4]. As a continuation of that project, we decided to exploit

our experience in the chemistry of *N*-aminoazoles [5–11] by preparing the *Schiff* bases **1**–**4** to study how the change in the nature of the substituent, heteroaromatic *vs.* aromatic, would affect the prototropic tautomerism of *Scheme 1*.

Moreover, the existence of additional H-bonding acceptors in the same molecule should modify the formation of the H-bonded network approaching what occurs in biological processes [12].

2. Results and Discussion. – The 4-[(1*H*-azol-1-ylimino)methyl] pyridin-3-ols **1**–**4** were prepared with good yields, by reaction of 3-hydroxypyridine-4-carboxaldehyde (**5**) with the corresponding 1*H*-azol-1-amines **6**–**9** [5] (*Scheme 2*).

Scheme 2

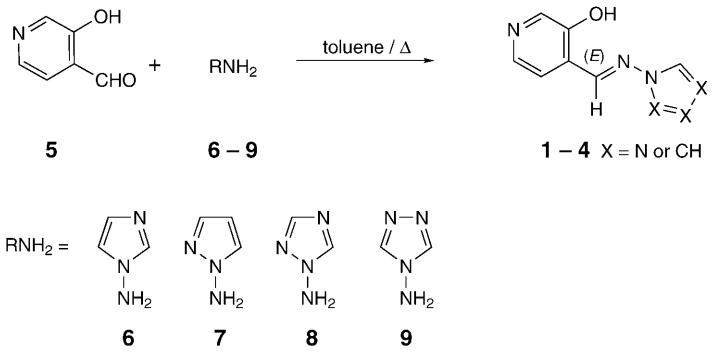

Although (*E*)- and (*Z*)-isomers could be formed in the reaction, only the (*E*)-form was detected in all cases, as established by 2D-NOESY-NMR experiments showing the correlation between the imino proton and H–C(5) of the pyridine ring, as well as with H–C(5′) of the azole moiety (or H–C(2′) in the cases of **1** and **4**) (*Sect. 2.2*). These results are in full agreement with B3LYP/6-31G** calculations that favor the (*E*)-isomer by 57.8 kJ mol^{-1} in compound **1** (from **6**), 46.7 kJ mol^{-1} in **2** (from **7**), 49.1 kJ mol^{-1} in **3** (from **8**) and 54.6 kJ mol^{-1} in **4** (from **9**). The same theoretical method was used to study the **A**/**B** tautomerism represented in *Scheme 1*: in the cases of compounds **1** and **4**, the **A** tautomer with (*E*)-configuration is more stable than **B** by *ca.* 50 kJ mol^{-1}. The presence of an N-atom in the α position of the azolyl moiety, such as in compounds **2** and **3**, further increases the difference in stability to the point that only tautomer **A** is a minimum. As we will show later on, these results are in agreement with the experimental observations.

The OH group of **1**–**4** can form an intramolecular H-bond with the N-atom, or intermolecular H-bonds with an N-atom of neighboring molecules. Moreover, there are 6 possible conformations for each **1**–**3** and 3 possible conformations for **4** due to rotations around the N–N, C–O, and C–C single bonds (*Fig. 1*). The results of the B3LYP/6-31G** calculations of the minimum energies of the various rotamers are summarized in *Table 1* showing that, in the case of isolated molecules in the gas phase, the **a** form presenting an intramolecular H-bond is always the most stable.

When looking at the azole moieties, only **2** and **3** have an N-atom at position N(2′), this being the reason why conformer **a** is favored. In compound **4**, conformers **a** and **b**, **c**

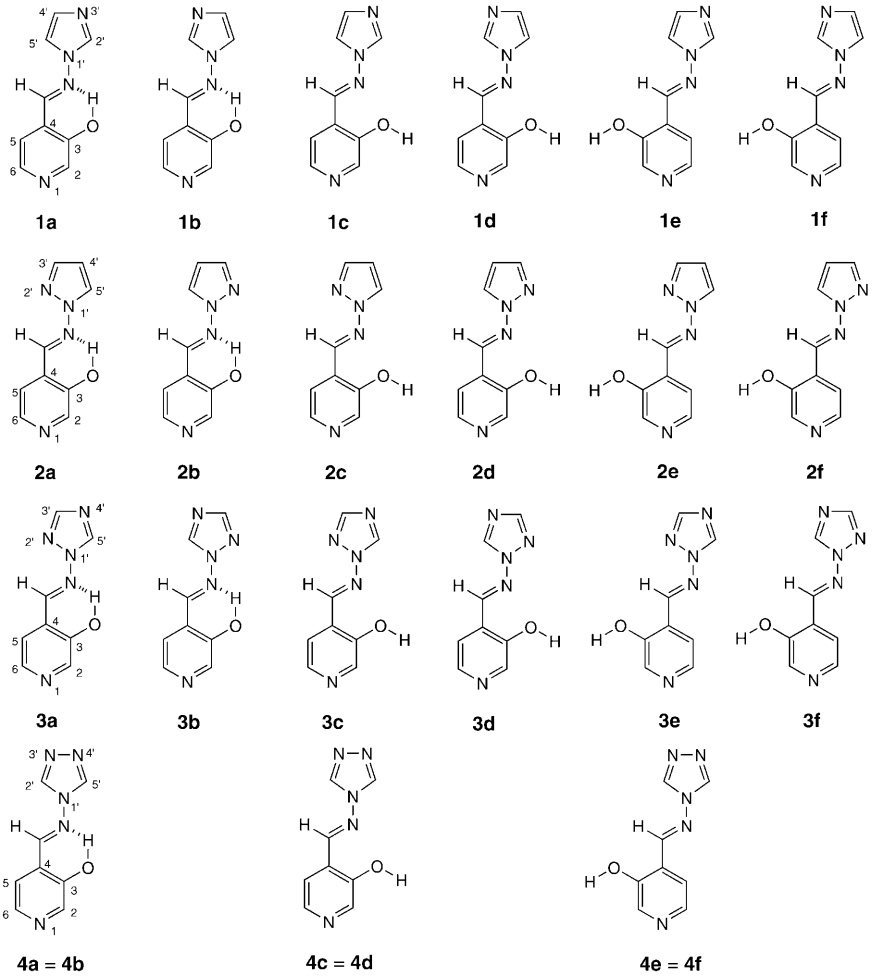

Fig. 1. *Calculated conformations for 4-{[*C(E)*]-(1*H*-azol-1-ylimino)methyl}pyridin-3-ols* **1**–**4** *with atom numbering*

and **d**, and **e** and **f** are pairwise identical, and finally in the imidazole derivative **1**, where all conformations are different, the relative stability order is **a** > **b** > **e** > **f** > **c** > **d** (*Table 1*). In other words, an N-atom in the β-position of the azolyl moiety (series **1**) prefers the s-*trans* conformation by *ca.* 4.5 kJ mol^{-1}, in the α-position (series **2**) favors the s-*cis* conformation by *ca.* 24.5 kJ mol^{-1}, and in case of N-atoms in both the α- and β-position (series **3**), the effects approximately add (*ca.* 26.0 kJ mol^{-1}).

2.1. *Crystal and Molecular Structures.* An X-ray study of all compounds was undertaken, but in the case of **2**, no appropriate crystals could be obtained. Crystals of **1**, **3**, and **4** consist in rotamers **e** interacting through intermolecular H-bonds, which led to different secondary structures. Selected bond distances and angles as well as the H-bond geometries are collected in *Table 2* and *3*, respectively.

Table 1. *Absolute Energies* [Hartree] *and Relative Energies* [kJ mol^{-1}]

		A	**b**	**c**	**d**	**e**	**f**
1		−641.9652 (0.0)	4.4	37.2	42.7	23.0	28.2
	+ZPE	−641.7985 (0.0)	4.0	35.0	40.0	21.2	25.9
2		−641.9584 (0.0)	23.01	38.5	68.0	26.8	51.2
	+ZPE	−641.7914 (0.0)	21.84	36.4	64.2	25.0	48.1
3		−658.0049 (0.0)	25.5	35.4	66.3	24.0	51.1
	+ZPE	−657.8493 (0.0)	23.8	33.3	63.2	22.3	47.6
4		−657.9832 (0.0)	0.0	34.2	34.2	20.3	20.3
	+ZPE	−657.8289 (0.0)	0.0	32.5	32.5	19.1	19.1

Table 2. *Selected Bond Lengths* [Å] *and Angles* [°] *for Compounds* **1**, **3**, *and* **4**

	1	**3**	**4**		**1**	**3**	**4**
C(1)–O(1)	1.355(3)	1.340(2)	1.344(2)	O(1)–C(1)–C(5)	119.3(2)	119.1(2)	119.7(2)
C(1)–C(5)	1.402(3)	1.398(2)	1.389(3)	C(5)–C(1)–C(2)	118.4(3)	118.6(2)	118.8(2)
C(1)–C(2)	1.394(3)	1.393(3)	1.388(3)	C(1)–C(5)–C(6)	120.3(2)	118.7(2)	120.4(2)
C(2)–N(1)	1.336(3)	1.334(2)	1.331(3)	C(6)–N(2)–N(3)	117.3(2)	116.1(2)	116.8(2)
C(3)–N(1)	1.347(3)	1.340(2)	1.341(3)	C(1)–O(1)–H(1)	107.5	113.1	112.1
C(3)–C(4)	1.367(3)	1.374(3)	1.377(3)	O(1)–C(1)–C(2)–N(1)	179.6(3)	−179.0(2)	−179.4(2)
C(4)–C(5)	1.396(3)	1.393(3)	1.401(3)	O(1)–C(1)–C(5)–C(4)	178.6(2)	178.2(2)	179.9(2)
C(5)–C(6)	1.468(3)	1.465(3)	1.461(3)	C(5)–C(6)–N(2)–N(3)	179.9(2)	179.1(2)	177.6(2)
C(6)–N(2)	1.281(3)	1.276(2)	1.271(3)	N(4)–C(7)–N(3)–N(2)	−179.3(2)	−179.3(2)	178.2(2)
N(2)–N(3)	1.387(3)	1.386(2)	1.396(2)	C(6)–N(2)–N(3)–C(9)	2.9(5)	–	–
				C(6)–N(2)–N(3)–C(7)	−179.3(2)	−178.5(2)	174.0(2)
				C(6)–N(2)–N(3)–N(5)	–	2.9(3)	–
				C(6)–N(2)–N(3)–C(8)	–	–	−9.2(4)

Table 3. *Data of Hydrogen Bonds of Compounds* **1**, **3**, *and* **4**

	D–H···A	δ(D–H) [Å]	δ(H···A) [Å]	δ(D···A) [Å]	<(DHA) [°]
1	O(1)–H(1)···N(4)[a])	1.09	1.59	2.666(3)	166.0
3	O(1)–H(1)···N(1)[b])	0.95	1.69	2.616(2)	164.3
4	O(1)–H(1)···O(2)	1.08	1.55	2.615(2)	168.7
	O(2)–H(2A)···N(1)[c])	0.98	1.92	2.858(2)	158.2
	O(2)–H(2B)···N(5)[d])	1.00	1.79	2.761(2)	163.4

Symmetry transformations used to generate equivalent atoms: [a]) $x-3/2,-y+1/2,z-1/2$. [b]) $1-x-1,y+1/2,-z+1/2$. [c]) $1-x+3,-y+2,-z+1$. [d]) $x+3/2,-y+3/2,z-1/2$.

Molecular drawings of **1**, **3**, and **4** are presented in *Figs. 2–4*. All molecules are almost planar with the maximum deviation for **4** (*Table 2*), and the geometries are in agreement with those calculated for the corresponding conformers.

The H-bond in **1** and **3** lead to zig-zag chains in the [203] and [010] directions, respectively. In compound **4** the intermolecular H-bonds involve a H_2O molecule,

forming layers parallel to the (103) plane. In the three cases, the analysis of the intermolecular distances shows that the chains in **1** and **3** and the layers in **4** are independent.

2.2. *NMR Studies.* We recorded the ^{1}H-NMR spectra (*Fig. 1* for atom numberings) of all four compounds **1**–**4** in (D_6)DMSO solution, and analysis of the chemical shifts (see *Table 4*) led to the conclusion that only the hydroxyimino form **A** exists in all cases in the solvent (D_6)DMSO. Except for **2**, the 4-{[*C*(*E*)]-(1*H*-azol-1-ylimino)methyl}pyridin-3-ols were not soluble in $CDCl_3$.

In the case of 1*H*-imidazol-1-ylimino derivative **1**, we detected in the NOESY plot the correlation of the imino proton with H–C(5′), H–C(2′), and H–C(5) as well as that of OH with H–C(2) thus establishing the disruption of the intramolecular H-bond (*Fig. 5*).

Only in $CDCl_3$, an intramolecular O–H···N=C H-bond was observed in the case of 1*H*-pyrazol-1-ylimino derivative **2** (*Fig 6*, *a*). In (D_6)DMSO, the NOESY plot (*Fig. 6*, *b*)

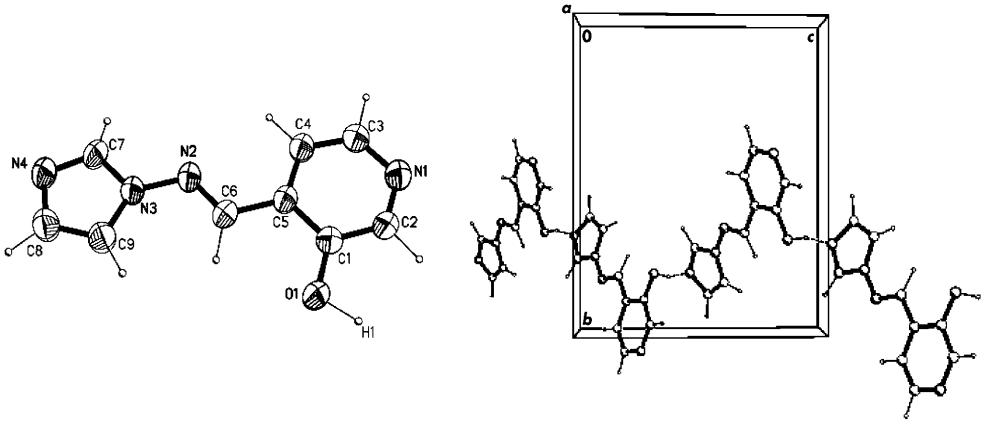

Fig. 2. *Molecular and crystal structures of* **1e**

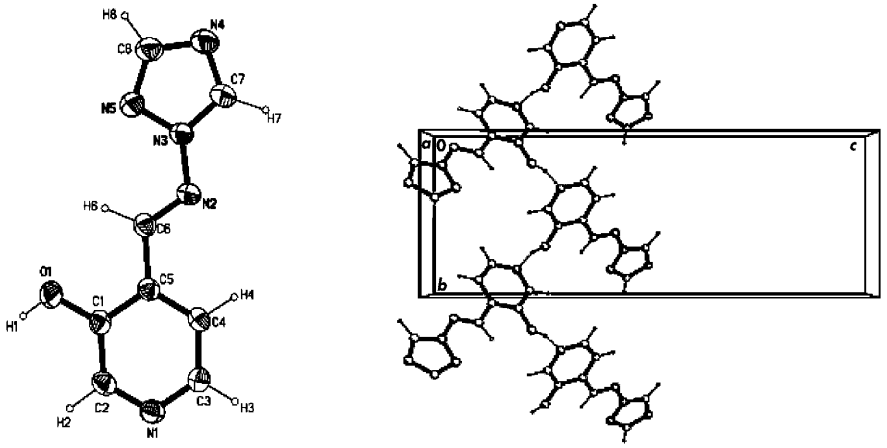

Fig. 3. *Molecular and crystal structures of* **3e**

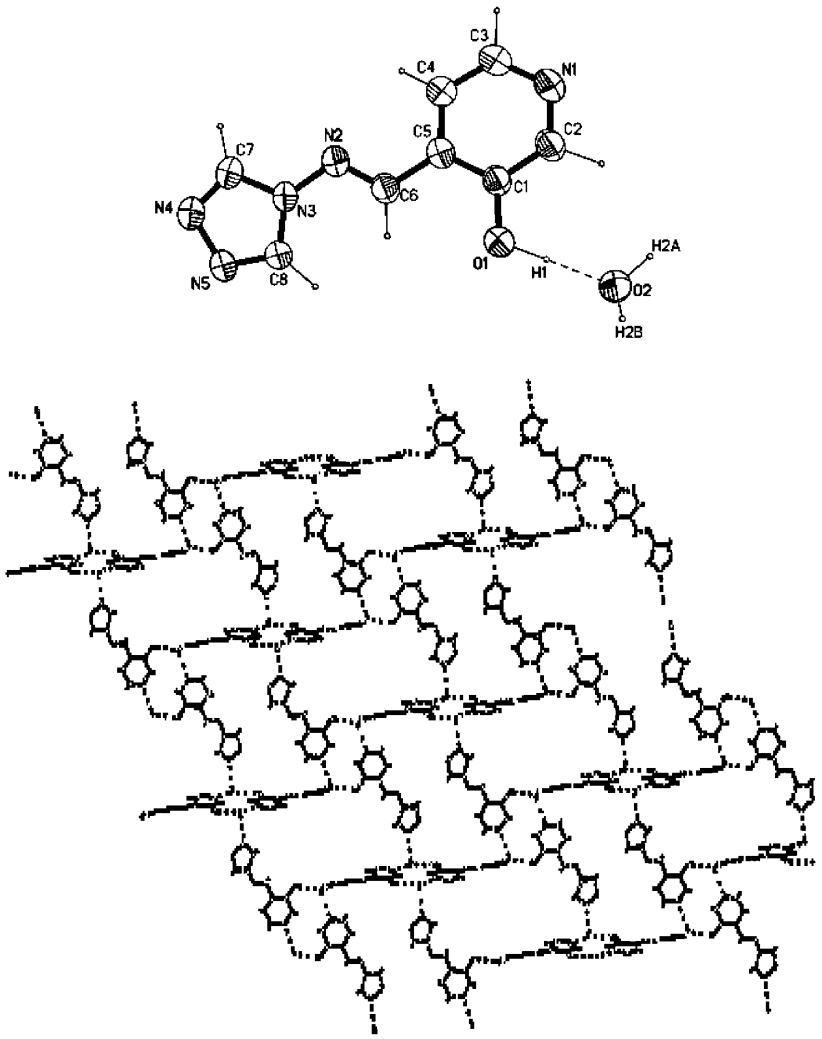

Fig. 4. *Molecular and crystal structures of* **4e**

Table 4. *^{1}H-NMR Chemical Shifts of the Iminomethylpyridinol Moiety.* δ in ppm.

	Solvent	CH=N	H–C(2)	OH	H–C(5)	H–C(6)
1	(D_6)DMSO	8.99	8.36	10.70	7.66	8.15
	CD_3OD	9.05	8.28	[a])	7.81	8.14
2	(D_6)DMSO	9.38	8.35	10.73	7.71	8.14
	$CDCl_3$	9.23	8.50	10.09	7.29	8.27
3	(D_6)DMSO	9.38	8.38	10.92	7.72	8.16
4	(D_6)DMSO	9.17	8.38	10.89	7.66	8.16

[a]) Replaced by OD.

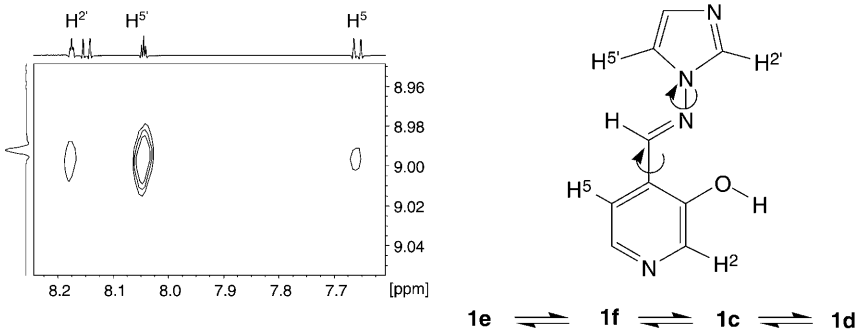

Fig. 5. *NOESY Plot* ((D$_6$)DMSO) *of 4-[[*C(E)*]-(1*H*-imidazol-1-ylimino)methyl]pyridin-3-ol* (**1**)

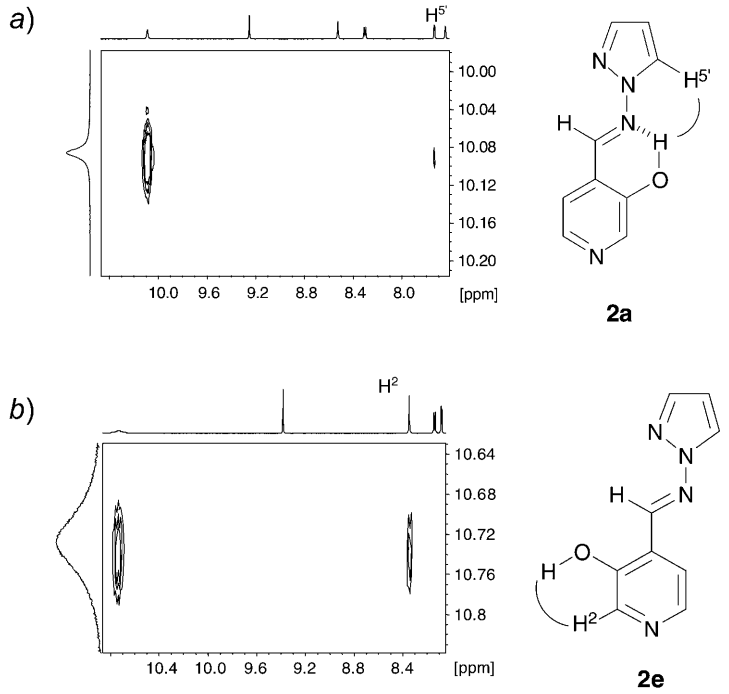

Fig. 6. *NOESY Plots of 4-[[*C(E)*]-(1*H*-pyrazol-1-ylimino)methyl]pyridin-3-ol* (**2**): a) *in CDCl$_3$ and* b) *in (D$_6$)DMSO*

revealed a correlation between H–C(2) and OH, indicating the absence of intramolecular H-bonds in such a polar solvent [13]. For **2**, the major changes of the ^{1}H-NMR data (*Table 4*) in going from $CDCl_3$ to (D$_6$)DMSO affected H–C(5) (δ 7.29 to 7.71) and the OH (δ 10.09 to 10.73).

In the case of the 1*H*-1,2,4-triazol-1-ylimino derivative **3**, no correlations involving the imino proton could be detected, and in the case of the 1*H*-1,3,4-triazol-1-ylimino

Table 5. *^{13}C-NMR Chemical Shifts and One-Bond Coupling Constants of the (Iminomethyl)pyridinol Moiety.* δ in ppm, ^1J in Hz.

		CH=N	C(2)	C(3)	C(4)	C(5)	C(6)
1	(D_6)DMSO	147.6 (J=170.5)	139.9 (J=179.1)	152.7	125.2	119.8 (J=163.8)	140.6 (J=181.1)
	CD_3OD	150.3	140.3	155.2	127.6	122.8	141.2
	CPMAS[a])	144.4	138.1	154.4	124.6	119.2	141.1
2	(D_6)DMSO	144.2 (J=172.2)	139.9 (J=176.5)	152.9.	125.0	119.1 (J=160.1)	140.4 (J=179.5)
	$CDCl_3$	150.3 (J=172.1)	140.8 (J=179.9)	152.8	122.2	124.0 (J=160.7)	141.2 (J=182.4)
	CPMAS[b])	140.7	138[h])	153.7	126.0	119.6	138[h])
		148.1		151.6	124.1	127.6	
	CPMAS[c])	140.0	138[h])	154.3	129.0	120.3	138[h])
3	(D_6)DMSO	147.8 (J=172.5)	140.1 (J=179.6)	153.1	124.2	119.1 (J=164.0)	140.5 (J=182.6)
	CPMAS[d])	146.0	139.3	153.7	122.9	120.7	143.3
	CPMAS[e])	147.4	143.0	155.9	124.0	119.9	143.0
			140.8	153.7	124.8		
					127.9		
4	(D_6)DMSO	152.1 (J=173.0)	140.1 (J=179.5)	152.9	124.5	119.5 (J=166.7)	140.5 (J=182.3)
	CPMAS[f])	148.4	135.4	154.1	124.6	120.7	144.2
	CPMAS[g])	152[h])	143[h])	155[h])	125[h])	121[h])	143[h])
		148[h])		152[h])	122[h])	119[h])	

[a]) Crystallized from toluene; δ 138.1 (C(2′)), 124.6 (C(4′)), 113.1 (C(5′)). [b]) Crystallized from EtOH/H_2O; δ 137.6 and 135.4 (C(3′)), 108.2 and 106.0 (C(4′)), 132.6 and 130.6 (C(5′)). [c]) Dissolved in $CHCl_3$ and evaporated; δ 134.0 (C(3′)), 110.3 (C(4′)), 129.3 (C(5′)). [d]) Crystallized from toluene; δ 149.9 and 149.5 (C(3′)), δ 138.0 (C(5′)). [e]) Crystallized from H_2O; δ 151.4 and 147.4 (C(3′)), δ 138.8 and 137.1 (C(5′)). [f]) Crystallized from H_2O; δ 138.4 (C(2′), C(5′)). [g]) Crystallized from $CHCl_3$/EtOH; δ 135.0 (C(2′), C(5′)). [h]) Broad signal.

derivative **4**, the NOESY experiments revealed a mixture of rotamers **4e** (=**4f**)/**4c** (=**4d**).

Solution ^{13}C-NMR studies (*Table 5*) showed signals for the C-atoms of the pyridine ring in agreement with the hydroxyimino structure (mean δ values: 150 (CH=N), 140 (C(2)), 153 (C(3)), 125 (C(4)), 119.5 (C(5)), and 140.5 (C(6)). The δ(C) for the azolyl substituents were within the normal ranges [5][7–9] (see *Exper. Part)*. The CH ^{13}C-NMR signals were found by gs-HMQC, and the quaternary C-atoms were assigned by long-range correlation experiments (gs-HMBC) [14]. In contrast to the *Schiff* bases we previously studied [4], the δ(C) of the C(6)s and their ^1J coupling constants (*Table 5*) were always larger than those of the C(2)s. For **2**, when changing from $CDCl_3$ to (D_6)DMSO, the most affected δ(C) (*Table 5*) were those of CH=N (δ 150.3 to 144.2) and of C(5) (δ 124.0 to 119.1), as expected for conformations **a** and **e**, respectively.

The ^{15}N-NMR solution data were obtained by gs-HMBC (*Table 6*). The signals furnishing more information about the tautomerism in the 4-[(1*H*-azol-1-ylimino)methyl]-pyridin-3-ols **1**–**4** are those of the CH=N moiety, which appeared between δ(N) −64.8 and −75.8 in (D_6)DMSO, *i.e.*, at values typical for the nonprotonated N-atom of a *Schiff* base [1–4]. They confirmed that compounds **1**–**4** exist in the hydroxyimino tautomeric form **A**.

Table 6. *^{15}N-NMR Chemical Shifts of* **1**–**4**. δ in ppm.

		CH=N	N(1)	N(1′)	N(2′)	N(3′)	N(4′)
1	(D_6)DMSO	−66.9	−52.9	−163.1		−120.8	
	CPMAS[a])	−67.3	−56.0	−160.2		−142.5	
2	(D_6)DMSO	−64.8	−53.1	−135.1	−94.5		
	$CDCl_3$	−78.2	−57.5	−141.7	−97.8		
	CPMAS[b])	−78.9	−55.6	−134.3	−95.7		
			−63.8	−136.8			
	CPMAS[c])	−85.7	−61.1	−133.5	−92.7		
3	(D_6)DMSO	−72.4	−50.5	−129.4	−103.6		−126.3
	CPMAS[a])	−74.2	−47.9	−126.3	−101.7		−138.9
	CPMAS[d])	−84.0	−63.5	−127.6	−101.3		−138.3
		−79.3		−122.5			
		−75.2					
		−71.9					
4	(D_6)DMSO	−75.8	−51.6	−164.9		−64.1	−64.1
	CPMAS[e])	−86.3	−65.2	−162.5		−82.7	−82.7
	CPMAS[d])	−75.7	55.2	−161.3		−71.7	−73.0
			59.7				

[a]) Crystallized from toluene. [b]) Crystallized from EtOH/H_2O. [c]) Dissolved in $CHCl_3$ and evaporated. [d]) Crystallized from H_2O. [e]) Crystallized from $CHCl_3$/EtOH.

The main results of the ^{13}C- and ^{15}N-CPMAS-NMR studies in the solid state, will be discussed for each derivative. Thus compound **1**, an **e** conformer, presented a single signal for each nucleus in the ^{13}C-CPMAS-NMR. As shown above, the X-ray structure of **1** confirmed the intermolecular associations involving the OH donor and the N(3′) acceptor, thus affording an explanation for the increase of the ^{15}N-NMR chemical shift (δ(solid) − δ((D_6)DMSO) = −21.7, see *Table 6*).

In the case of **2**, we did not succeed in growing suitable crystals for X-ray studies. Therefore, the solid-state NMR conclusions could not be confirmed by the X-ray structure. When **2** was dissolved in $CHCl_3$ and then the solution rapidly evaporated prior to the recording of the ^{13}C-CPMAS-NMR spectrum (*Fig. 7*, *a*, NQS (non-quaternary suppression), and *Fig. 7*, *b*), only one structure was observed, most probably the one that presents the intramolecular H-bond, conformation **2a**. When **2** crystallized from an EtOH/H_2O mixture, two different rotamers **2a** and **2e** coexisted. This was clearly apparent from the C(3) and C(4) signals of the pyridine ring (*Fig. 7*, *c*, NQS) and C(4′) of the pyrazole moiety (*Fig. 7*, *d*). The **2a** form evolved towards a mixture of **2a** and **2e** on standing.

The ^{13}C-CPMAS-NMR spectrum of **3** obtained from toluene showed the presence of only structure **3e**, but in the spectrum registered after recrystallization from H_2O at least three distinct signals for C(4) were observed, attributable to the presence of other rotamers.

Crystals of **4** from H_2O corresponded to conformation **e**, but those obtained from $CHCl_3$/EtOH afforded two types of molecules, **4e** and **4c**, as clearly observed in the splitting of C(3) and C(4) in the ^{13}C-CPMAS-NMR spectra.

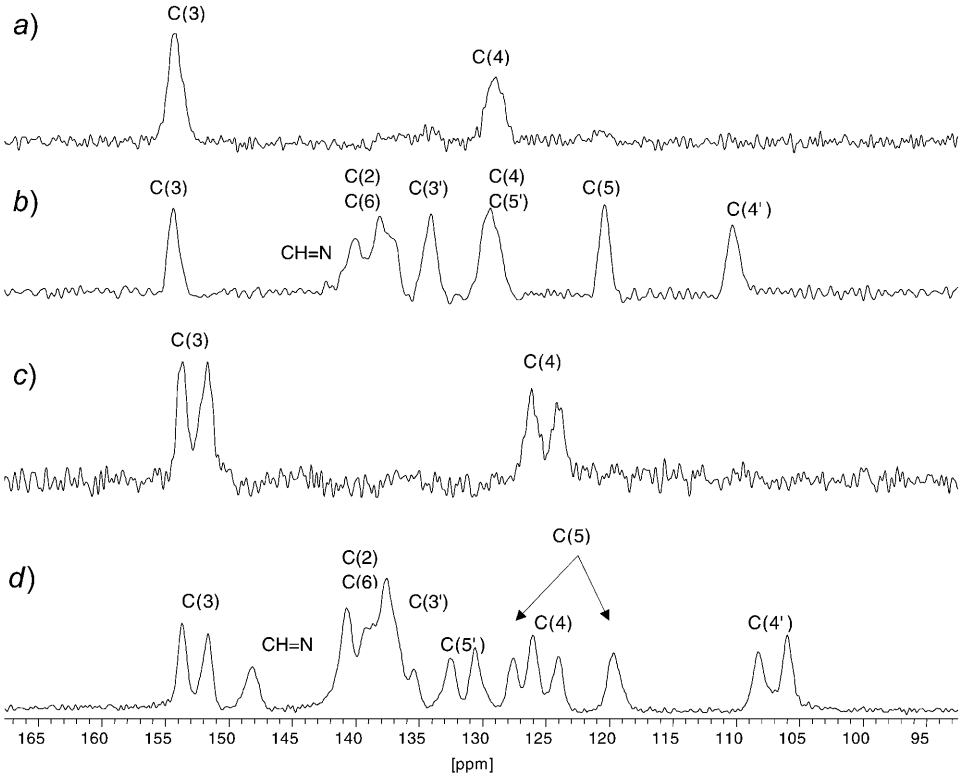

Fig. 7. *^{13}C-CPMAS-NMR Spectra of compound* **2**

3. Conclusions. – The structure of *Schiff* bases derived from 3-hydroxypyridine-4-carboxaldehyde and four 1*H*-azol-1-amines was determined in the solid state (X-ray crystallography and CPMAS-NMR) and in solution (NMR and DFT calculations). Concerning tautomerism and *E/Z* isomerism about the C–N bond, all of them have the hydroxyimino structure with (*E*)-configuration. On the other hand, the conformation about the N–N and C–O single bonds strongly depends on the phase and the nature of the azolamine. In particular, in the solid state, O–H···N intermolecular H-bonds are always preferred to intramolecular ones.

This work was supported by *DGES/MCyT* (Project no. BQU2003-00976). One of us (*A. P.*) is indebted to the *MCyT* of Spain for an *FPI* grant.

Experimental Part

General. M.p.: under a microscope *Axiolab Zeiss* with a *TMS-92-Linkan* heating stage and by DSC with a *Seiko DSC 220C* connected to a *SSC5200H* disk station; thermograms: sample size 0.003–0.010 g, scanning rate 2.0° min^{-1}. TLC: aluminium-backed plates of silica gel *60 F_{254}* (*Merck*, 0.2 mm). Elemental analyses: *Perkin-Elmer-240* apparatus; performed by the 'Centro de Microanálisis Elemental-UCM', Madrid.

NMR Spectroscopy [14]. Solution NMR spectra: *Bruker-DRX-400* (9.4 Tesla, 400.13 MHz for ^{1}H, 100.62 MHz for ^{13}C and 40.56 MHz for ^{15}N) spectrometer with a 5-mm inverse-detection H–X probe equipped with a *z*-gradient coil, at 300 K; chemical shifts δ in ppm rel. to the internal solvent $CDCl_3$ (δ(H) 7.26 and δ(C) 77.0), (D_6)DMSO (δ(H) 2.49 and δ(C) 39.5), or CD_3OD (δ(H) 3.31 and δ(C) 49.2) and rel. to the external standard nitromethane (δ(N) 0.00). Typical parameters for ^{1}H-NMR spectra: spectral width 4000 Hz, pulse width 7.5 μs, attenuation level 0 dB, resolution 0.15–0.25 Hz per point. Typical parameters for ^{13}C-NMR spectra: spectral width 21 kHz, pulse width 10.6 μs, attenuation level −6 dB, resolution 0.6 Hz per point, relaxation delay 2 s; WALTZ-16 was used for broadband proton decoupling; the FIDs were multiplied by an exponential weighting (*lb* = 2 Hz) before *Fourier* transformation. 2D ^{1}H,^{1}H-gs-COSY and inverse proton-detected heteronuclear shift-correlation spectra, ^{1}H,^{13}C-gs-HMQC, ^{1}H,^{13}C-gs-HMBC, and ^{1}H,^{15}N-gs-HMBC, were acquired and processed by using standard *Bruker* NMR software and in non-phase-sensitive mode. Gradient selection was achieved through a 5% sine truncated shaped pulse gradient of 1 ms. Selected parameters for ^{1}H,^{1}H-gs-COSY: spectral width 2500–3500 Hz, acquisition data size 1024 points, one transient accumulated per increment, relaxation delay 1 s, a total of 256 experiments, data processing by using zero filling in the *F*1 domain and shifted sine-bell apodization of factor 0 in both dimensions. Selected parameters for ^{1}H,^{1}H-gs-NOESY: spectral width 2000–3000 Hz, acquisition data size 1024 points, 32 transients accumulated per increment, relaxation delay 1 s, mixing time 750–1800 ms, a total of 512 experiments, data processing by using zero filling in the *F*1 domain and shifted sine-bell apodization of factor 0 in both dimensions. Selected parameters for ^{1}H,^{13}C-gs-HMQC and gs-HMBC spectra: spectral width 2500–3500 Hz for ^{1}H and 12.0–20.5 kHz for ^{13}C, 1024 × 256 data set, number of scans 2 (gs-HMQC), or 4 (gs-HMBC), and relaxation delay 1s. The FIDs were processed by using zero filling in the *F*1 domain and a sine-bell window function in both dimensions was applied prior to *Fourier* transformation. In the gs-HMQC experiments, GARP modulation of ^{13}C was used for decoupling. Selected parameters for ^{1}H,^{15}N-gs-HMBC spectra: spectral width 2500–3500 Hz for ^{1}H and 12.5 kHz for ^{15}N, 1024 × 256 data set, number of scans 4, relaxation delay 1s, 37–75 ms delay for the evolution of the ^{15}N,^{1}H long-range coupling. The FIDs were processed by using zero filling in the *F*1 domain, and a sine-bell window function in both dimensions was applied prior to *Fourier* transformation.

Solid-state ^{13}C- and ^{15}N-CPMAS-NMR spectra: *Bruker-WB-400* spectrometer at 100.73 (^{13}C) and 40.60 MHz (^{15}N) and 300 K with a 4 mm *DVT* probehead. Samples were carefully packed in a 4-mm-diameter cylindrical zirconia rotor with Kel-F end-caps. Operating conditions involved 3.2 μs 90° ^{1}H pulses and decoupling field strength of 78.1 kHz by TPPM sequence. The ^{13}C spectra were originally referenced to a glycine sample and then the δ(C) were recalculated rel. to Me_4Si (carbonyl atom of glycine: δ 176.1). The ^{15}N spectra were originally referenced to $^{15}NH_4Cl$ and then converted to the nitromethane scale *via* the relationship $\delta(Me^{15}NO_2) = \delta(^{15}NH_4Cl) - 338.1$. Typical acquisition parameters for ^{13}C-CPMAS-NMR: spectral width 40 kHz, recycle delay 60–120 s, acquisition time 30 ms, contact time 2–6 ms, and spin rate 12 kHz. To distinguish protonated and unprotonated C-atoms, the NQS (non-quaternary suppression) experiment by conventional cross-polarization was recorded; before the acquisition, the decoupler was switched off for a very short time of 25 μs [15][16]. Typical acquisition parameters for ^{15}N-CPMAS-NMR: spectral width 40 kHz, recycle delay 60–120 s, acquisition time 35 ms, contact time 8 ms, and spin rate 6 kHz.

DFT Calculations. The optimization of the structures of all compounds discussed in this paper was carried out at the hybrid B3LYP/6-31G** level [17][18] with basis sets of Gaussian-type functions by using Spartan '02 for Windows [19].

Syntheses. Compounds **1**–**4** were prepared by refluxing in toluene equimolar amounts of **5** [4] and the corresponding amine **6**–**9** [5] during 7 h and stirring overnight: yield 85–90%.

*4-{[C(*E*)]-(1*H*-Imidazol-1-ylimino)methyl}pyridin-3-ol* (**1**). TLC ($CHCl_3$/EtOH 9:1): R_f 0.31. The crystals were purified by crystallization (C_7H_8). M.p. 251.4° (dec; DSC); under the microscope, **1** changed its appearance at 219° decomposing at 263°. ^{1}H-NMR ((D_6)DMSO): 10.70 (br. *s*, OH); 8.99 (*s*, CH=N); 8.36 (*s*, H–C(2)); 8.17 (*t*, $^4J(2',4') = {}^4J(2',5') = 1.3$, H–C(2′)); 8.15 (*d*, $^3J(5,6) = 5.0$, H–C(6)); 8.04 (*t*, $^3J(4',5') = {}^4J(2',5') = 1.3$, H–C(5′)); 7.66 (*d*, H–C(5)); 7.07 (*t*, H–C(4′)). ^{13}C-NMR ((D_6)DMSO): 152.7 ($^3J = {}^3J = 4.7$, C(3)); 147.6 ($^1J = 170.5$, $^3J = 4.5$, CH=N); 140.6 ($^1J = 181.1$, $^3J = 10.9$, C(6)); 139.9 ($^1J = 179.1$, $^3J = 11.2$, C(2)); 136.4 ($^1J = 213.6$, C(2′)); 128.8 ($^1J = 190.7$, $^3J = 11.8$, $^2J = 9.3$, C(4′)); 125.2 (C(4)); 119.8 ($^1J = 163.8$, $^3J = 9.5$, $^2J = 3.5$, C(5)); 112.8 ($^1J = 195.6$, $^3J = 2.7$, $^2J = 16.9$, C(5′)). ^{1}H-NMR

(CD_3OD): 9.05 (*s*, CH=N); 8.28 (*s*, H–C(2)); 8.18 (*t*, $^4J(2',4')=^4J(2',5')=1.4$, H–C(2′)); 8.14 (*d*, $^3J(5,6)=5.1$, H–C(6)); 7.92 (*t*, $^3J(4',5')=1.4$, H–C(5′)); 7.81 (*d*, H–C(5)); 7.13 (*t*, H–C(4′)). ^{13}C-NMR (CD_3OD): 155.2 (C(3)); 150.3 (CH=N); 141.2 (C(6)); 140.3 (C(2)); 138.0 (C(2′)); 129.6 (C(4′)); 127.6 (C(4)); 122.8 (C(5)); 113.6 (C(5′)). Anal. calc. for $C_9H_8N_4O$: C 57.44, H 4.28, N 29.77; found: C 57.35, H 4.34, N 29.84.

*4-{[C(*E*)]-(1*H*-Pyrazol-1-ylimino)methyl}pyridin-3-ol* (**2**). TLC ($CHCl_3$/EtOH 9:1): R_f 0.79. The crystals were purified by crystallization ($CHCl_3$). M.p. 163° (microscope) and 164.4° (DSC). ^{1}H-NMR ((D_6)DMSO): 10.73 (br. *s*, OH); 9.38 (*q*, $^4J(CH,5)=0.7$, $^5J(CH,6)=0.7$, $^6J(CH,3')=0.7$, CH=N); 8.35 (*dd*, $^4J(2,6)=0.4$, $^5J(2,5)=0.6$, H–C(2)); 8.14 (*ddd*, $^3J(5,6)=5.0$, H–C(6)); 8.08 (*dd*, $^3J(4',5')=2.5$, $^4J(3',5')=0.8$ H–C(5′)); 7.71 (*t*, H–C(5)); 7.68 (*td*, $^3J(4',3')=1.9$, H–C(3′)); 6.51 (*dd*, H–C(4′)). ^{13}C-NMR ((D_6)DMSO): 152.9 (C(3)); 144.2 ($^1J=172.2$, CH=N); 140.4 ($^1J=179.5$, C(6)); 139.9 ($^1J=176.5$, C(2)); 138.5 ($^1J=187.8$, C(3′)); 129.9 ($^1J=195.0$, C(5′)); 125.0 (C(4)); 119.1 ($^1J=160.1$, C(5)); 107.0 ($^1J=178.7$, C(4′)). ^{1}H-NMR ($CDCl_3$): 10.09 (br. *s*, OH); 9.23 (*d*, $^6J(CH,3')=0.8$, CH=N); 8.50 (*s*, H–C(2)); 8.27 (*d*, $^3J(5,6)=4.9$, H–C(6)); 7.71 (*dd*, $^3J(4',5')=2.5$, $^4J(3',5')=0.8$, H–C(5′)); 7.62 (*td*, $^3J(3',4')=1.9$, H–C(3′)); 7.29 (*d*, H–C(5)); 6.45 (*dd*, H–C(4′)). ^{13}C-NMR ($CDCl_3$): 152.8 (C(3)); 150.3 ($^1J=172.1$, $^3J=6.4$, CH=N); 141.2 ($^1J=182.4$, $^3J=10.1$, C(6)); 140.8 ($^1J=179.9$, $^3J=10.4$, C(2)); 139.0 ($^1J=188.3$, $^3J=9.1$, $^2J=5.4$, C(3′)); 129.0 ($^1J=192.4$, $^3J=3.7$, $^2J=8.8$, C(5′)); 124.0 ($^1J=160.7$, $^3J=9.1$, C(5)); 122.2 (C(4)); 107.5 ($^1J=179.8$, $^2J=^2J=8.8$, C(4′)). Anal. calc. for $C_9H_8N_4O$: C 57.44, H 4.28, N 29.77; found: C 57.30, H 4.68, N 27.71.

Table 7. *Crystal Data and Structure Refinement for Compounds* **1**, **3**, *and* **4**

	1	**3**	**4**
Identification code	CCDC-285402	CCDC-285403	CCDC-285404
Empirical formula	$C_9H_8N_4O$	$C_8H_7N_5O$	$C_8H_9N_5O_2$
Formula weight	188.19	189.19	207.20
Crystal system	Monoclinic	Monoclinic	Monoclinic
Space group	*P*2(1)/*n*	*P*2(1)/*c*	*P*2(1)/*n*
Unit cell dimensions			
a [Å]	5.2731(8)	4.6828(6)	4.8932(5)
b [Å]	14.389(2)	8.488(1)	22.033(2)
c [Å]	11.677(2)	21.990(3)	9.169(1)
β [°]	93.735(4)	90.308(3)	97.697(2)
Volume [Å^3]	884.1(2)	874.0(2)	979.6(2)
Z	4	4	4
Density (calculated) [Mg/m^3]	1.414	1.438	1.405
Absorption coefficient [mm^{-1}]	0.099	0.104	0.106
F(000)	392	392	432
Scan Technique	*ω* and *φ*	*ω* and *φ*	*ω* and *φ*
θ range for data collection [°]	2.25 to 24.99	1.85 to 24.99	1.85 to 24.99
Index ranges	$-6\le h\le 6$	$-5\le h\le 5$	$-5\le h\le 5$
	$-17\le k\le 16$	$-10\le k\le 10$	$-23\le k\le 26$
	$-7\le l\le 13$	$-17\le l\le 26$	$-8\le l\le 10$
Reflections collected	4549	4418	5031
Independent reflections	1553 (R(int) = 0.072)	1541 (R(int) = 0.0442)	1716 (R(int) = 0.0462)
Data, restraints, parameters	1553, 0, 136	1541, 0, 134	1716, 0, 145
Reflections observed ($I>2\sigma(I)$)	749	1011	1014
Goodness-of-fit on F^2	0.913	0.931	0.923
R[a]) [observed reflec.]	$R_1=0.0447$	$R_1=0.0396$	$R_1=0.0421$
Rw_F[b]) (all data)	$wR_2=0.1078$	$wR_2=0.1018$	$wR_2=0.1089$

[a]) $\Sigma||F_o|-|F_c||/\Sigma|F_o|$. [b]) $\{\Sigma[w(F_o^2-F_c^2)^2]/\Sigma[w(F_o^2)^2]\}^{1/2}$.

*4-{[C(*E*)]-(1*H*-1,2,4-Triazol-1-ylimino)methyl}pyridin-3-ol* (**3**). TLC ($CHCl_3$/EtOH 9:1): R_f 0.55. The crystals were purified by crystallization ($CHCl_3$/EtOH). M.p. 230° (microscope), and 236.6° with decomposition at 263.6° (DSC). ^{1}H-NMR ((D_6)DMSO): 10.92 (br. *s*, OH); 9.38 (*s*, CH=N); 8.99 (*s*, H–C(5′)); 8.38 (*s*, H–C(2)); 8.20 (*s*, H–C(3′)); 8.16 (*d*, ^3J(5,6) = 5.0, H–C(6)); 7.72 (*d*, H–C(5)). ^{13}C-NMR ((D_6)DMSO): 153.1 (C(3)); 150.0 (^1J = 211.1, ^3J = 12.4, C(3′)); 147.8 (^1J = 172.5, ^3J = 3.6, CH=N); 140.5 (^1J = 182.6, ^3J = 10.9, C(6)); 140.1 (^1J = 179.6, ^3J = 11.2, C(2)); 134.1 (^1J = 218.7, ^3J = 6.5, C(5′)); 124.2 (^3J = ^3J = ^2J = 6.3, C(4)); 119.1 (^1J = 164.0, ^3J = 9.9, ^2J = 4.2, C(5)). Anal. calc. for $C_8H_7N_5O$: C 50.79, H 3.73, N 37.02; found: C 50.07, H 4.01, N 35.35.

*4-{[C(*E*)]-(1*H*-1,3,4-Triazol-1-ylimino)methyl}pyridin-3-ol* (**4**). TLC ($CHCl_3$/EtOH 9:1): R_f 0.11. The crystals were purified by crystallization (H_2O/EtOH). M.p. 280° (microscope) and 240° (dec.; DSC). ^{1}H-NMR ((D_6)DMSO): 10.89 (br. *s*, OH); 9.23 (*s*, H–C(2′), H–C(5′)); 9.17 (*s*, CH=N); 8.38 (*s*, H–C(2)); 8.16 (*d*, ^3J(5,6) = 5.0, H–C(6)); 7.66 (*d*, H–C(5)). ^{13}C-NMR ((D_6)DMSO): 152.9 (C(3)); 152.1 (^1J = 173.0, CH=N); 140.5 (^1J = 182.3, ^3J = 11.4, C(6)); 140.1 (^1J = 179.5, ^3J = 11.3, C(2)); 139.1 (^1J = 216.1, ^3J = 3.3, C(2′), C(5′)); 124.5 (C(4)); 119.5 (^1J = 166.7, C(5)). Anal. calc. for $C_8H_7N_5O.H_2O$: C 46.38, H 4.38, N 33.80; found: C 46.47, H 4.41, N 34.00.

X-Ray Data Collection and Structure Refinement. Suitable crystals for X-ray diffraction experiments were obtained by crystallization from H_2O/EtOH. Data collection for compounds were carried out at r.t. with a *Bruker-Smart-CCD* diffractometer by using graphite-monochromated Mo-K_α radiation (λ 0.71073 Å) operating at 50 kV and 30 mA. In all cases, data were collected over a hemisphere of the reciprocal space by combination of three exposure sets. Each exposure of 30s covered 0.3 in ω. The cell parameter were determined and refined by a least-squares fit of all reflections. A summary of the fundamental crystal and refinement data of **1**, **3**, and **4** is given in *Table 7*. The structures were solved by direct methods (SHELXS-97) and refined by full-matrix least-square procedures on F^2 (SHELXL-97) [20]. All non-H-atoms were refined anisotropically. All H-atoms were located on a difference *Fourier* map and refined riding on the respective C- or O-atoms. Largest peaks and holes in the final difference map were 0.165 and −0.150, 0.175 and −0.178, 0.154 and −0.151 e Å^{-3} for **1**, **3**, and **4**, respectively.

CCDC-285402, CCDC-285403, and CCDC-285404 contain the supplementary crystallographic data for this paper. These data can be obtained free of charge *via* http://www.ccdc.cam.ac.uk/data_request/cif from the *Cambridge Crystallographic Data Centre.*

REFERENCES

[1] S. H. Alarcón, A. C. Olivieri, D. Sanz, R. M. Claramunt, J. Elguero, *J. Mol. Struct.* **2004**, *705*, 1.
[2] Q. T. That, K. P. P. Nguyen, P. E. Hansen, *Magn. Reson. Chem*. **2005**, *43*, 302.
[3] A. Filarowski, A. Koll, T. Glowiak, E. Majewski, T. Dziembowska, *Ber. Bunsenges. Phys. Chem*. **1998**, *102*, 393.
[4] D. Sanz, A. Perona, R. M. Claramunt, J. Elguero, *Tetrahedron* **2005**, *61*, 145.
[5] M. C. Foces-Foces, F. Hernández-Cano, R. M. Claramunt, D. Sanz, J. Catalán, F. Fabero, A. Fruchier, J. Elguero, *J. Chem. Soc., Perkin Trans. 2* **1990**, 237.
[6] J. L. Aubagnac, R. M. Claramunt, D. Sanz, *Org. Mass Spectrom. Lett.* **1990**, *25*, 293.
[7] L. Salazar, M. Espada, C. Avendaño, R. M. Claramunt, D. Sanz, J. Elguero, *J. Org. Chem.* **1992**, *57*, 1563.
[8] R. M. Claramunt, D. Sanz, J. Catalán, F. Fabero, N. A. García, C. Foces-Foces, A. Llamas-Saiz, J. Elguero, *J. Chem. Soc., Perkin Trans. 2* **1993**, 1687.
[9] A. F. Pozharski, V. V. Kuzmenko, C. Foces-Foces, A. L. Llamas-Saiz, R. M. Claramunt, D. Sanz, J. Elguero, *J. Chem. Soc., Perkin Trans. 2* **1994**, 841.
[10] R. M. Claramunt, D. Sanz, J. Elguero, *An. Asoc. Quím. Argentina* **2001**, *89*, 15.
[11] D. Sanz, J. A. Jiménez, R. M. Claramunt, J. Elguero, *Arkivoc* **2004**, *5*, 100.
[12] G. Zundel, *Adv. Chem. Phys.* **2000**, *111*, 1.
[13] C. Reichardt, 'Solvents and Solvents Effects in Organic Chemistry', 2nd edn., VCH, Weinheim, 1988.
[14] S. Berger, S. Braun, '200 and more NMR Experiments', Wiley-VCH, Weinheim, 2004.
[15] P. D. Murphy, *J. Magn. Reson*. **1983**, *52*, 343; *J. Magn. Reson.* **1985**, *62*, 303.

[16] L. B. Alemany, D. M. Grant, T. D. Alger, R. J. Pugmire, *J. Am. Chem. Soc.* **1983**, *105*, 6697.
[17] A. D. Becke, *Phys. Rev. A* **1988**, *38*, 3098; A. D. Becke, *J. Chem. Phys.* **1993**, *98*, 5648; C. Lee, W. Yang, R. G. Parr, *Phys. Rev. B* **1988**, *37*, 785; B. Miehlich, A. Savin, H. Stoll, H. Preuss, *Chem. Phys. Lett*. **1989**, *157*, 200.
[18] P. C. Hariharan, J. A. Pople, *Theor. Chim. Acta* **1973**, *28*, 213.
[19] 'Spartan 2002 for Windows', from Wavefunction Inc.
[20] G. M. Sheldrick, 'SHELX97, Program for Refinement of Crystal Structure', University of Göttingen, Göttingen, Germany, 1997.

Received January 31, 2006